Fluidic Thrust Vectoring: CFD Analysis of Secondary Injection in Convergent-Divergent Nozzles

Deepak Gupta[1*], Bhavesh Jindal[2], Swati Gill[2]

[1] *Assistant Professor, Department of Aerospace, GNA University Phagwara, India 144401*

[2] *Undergraduate Student, Department of Aerospace, GNA University Phagwara, India 144401*

**Corresponding Author- Deepak.gupta@gnauniversity.edu.in*

Abstract

Secondary flow injection for thrust vectoring offers a simple alternative to mechanical thrust vectoring systems by redirecting the exhaust flow, without using any moving parts. This study conducts a computational fluid dynamics (CFD) analysis of secondary injection in an axisymmetric convergent–divergent (C–D) nozzle with ANSYS Fluent 2025 R2. A density based solver with the SST k–ω turbulence model was utilized for assessing the application of a nozzle pressure ratio (NPR = 2.67) and secondary pressure ratio (SPR = 1.05) on flow behavior and vectoring performance while using the converging nozzle as the injection area. The results show that secondary injection results in the formation of asymmetric flow structures and oblique shock in the divergent section with a maximum Mach number of 1.72 and jet deflection angle of ≈6.8° and thrust loss less than 3 %. The static pressure ratio in the vicinity of the injector region was approximately (≈1.05–1.07) is similar to previous studies, indicating that the numerical model is accurate. The findings of this study support that secondary injection increases thrust control and maneuverability while decreasing structural complexity, indicating that fluidic thrust vectoring can provide a potential technology for future Unmanned Aerial Vehicle (UAV), missiles, and supersonic aircraft propulsion system.

Keywords- Fluidic thrust vectoring, secondary flow injection, Convergent–divergent nozzle, Supersonic flow, Computational fluid dynamics (CFD), Shock vector control, ANSYS Fluent

Introduction

Numerous studies have appeared in the literature regarding secondary flow injection and fluidic thrust vectoring characteristics in convergent–divergent (CD) nozzles, primarily in the context of advanced propulsion systems [1]. Fluidic thrust vectoring is characterized by the injection of a secondary airflow into the divergent section of a nozzle, producing an overall effective vectoring deflection of the exhaust jet with high controllable thrust directionality (without using mechanically movable parts). The fundamental concept of fluidic thrust vectoring can be traced back to the mid-20th Century with its origins generally attributed to missile systems; however, the adoption of this relatively emerging technology has been facilitated as computational fluid dynamics (CFD) modeling and experimental validation capabilities improved [2].

Extensive studies have investigated the deflection of the jet and the overall fluidic thrust vectoring efficiency by investigating key characteristics including the nozzle pressure ratio (NPR), secondary pressure ratio (SPR), injection type (type of geometry), and injection location [3]. Recent numerical and experimental studies particularly with simulation platforms such as ANSYS Fluent, show fluidic injected thrust vectoring has substantial benefits, including reductions in overall system weight, stealthiest, and overall reliability in comparison to mechanically controlled thrust vectoring systems [4]. This study investigates secondary injection mechanisms in an axisymmetric pipe, methodically assessing how changes in injection parameters impact thrust vectoring authority and overall performance. The aligned exhaust flow, directed down the nozzle axis, creates longitudinal thrust and increases maneuverability. Therefore, it provides increased control authority over a wide spectrum of flight regimes—especially at high angle of attack and unsteady low-speed flight conditions. In this regard, fluidic thrust vectoring enhances adaptability and controllability in regions where aerodynamic surfaces are less effective [5]. Fluidic thrust vectoring

mechanisms can generally be classified into three categories: Shock Vector Control (SVC), Throat Shifting (TS) and Counter flow Injection [6]. Of these mechanisms, SVC has been the most extensively studied and evaluated over various nozzle model designs and configurations because of its ability to modify shock structures for the purpose of jet deflection. More broadly, all thrust vectoring mechanisms can be categorized into four types: (i) mechanical deflection of the thrust chamber or nozzle using movable or gimbaled mechanisms; (ii) deflection using heat-resistant moveable bodies such as jet vanes or jetavators inserted in the exhaust flow; (iii) asymmetric flow distortion using injection of a secondary fluid; and (iv) auxiliary thrust chambers that create thrust vectoring forces independent of the primary nozzle flow [7]. Thrust vectoring is considered a potential technology for next-generation supersonic aircraft. It not only helps meet performance requirements for takeoff and landing but also allows for design freedom for low–sonic-boom configurations [8]. Properly tuning lift distribution with thrust vectoring can mitigate the intensity of a sonic boom and improve cruise performance. Thrust vectoring can also be used as a complementary control power source to augment traditional aerodynamic control surfaces during trimming processes, thus reducing cruise trim drag. In low dynamic pressures, when traditional control surfaces are significantly less effective, thrust vectoring serves as a critical control mechanism. Thrust vectoring is generally categorized by two different means- mechanical thrust vectoring (MTV) characterized by adjustable nozzles or physical aerodynamic devices, or fluidic thrust vectoring (FTV) typically attributed to controlled secondary injection manipulating the direction of the exhaust flow [9]. Mechanical means work well but fluidic applications have a few advantages such as decreased mechanical complexity, less structural mass, and increased stealth capability. Future studies should prioritize the use of reactive and inert secondary injection fluids to improve performance and efficiency [10]. The integration of fluidic applications in propulsion systems with thrust vectoring provides aerodynamic efficiency and performance, increases fuel efficiency, and augment maneuverability and safety. Consequently, fluidic thrust vectoring represents a critical advancement in modern and future aerospace propulsion technologies.

2. Literature Review

Extensive research has been conducted on secondary injection and fluidic thrust vectoring in convergent–divergent (C–D) nozzles and related propulsion systems. This section reviews key numerical and experimental studies, emphasizing methods, results, and trends relevant to fluidic thrust vectoring.

2.1 **Flow Behavior and Secondary Injection Effects**

In a numerical study, Yang *et al.* investigated the flow field of a 3D over–under TBCC exhaust nozzle during turbojet-only operation. They showed that secondary jet injection forms a *virtual exit plane* tilted relative to the stream wise axis, causing deflection of the core jet and alteration of the thrust vector (vectored thrust) [1]. They also observed that the vectoring angle increases with secondary jet momentum until a limit, and that vectoring raises the static pressure at the nozzle entrance, which correlates with improved engine performance.

Chandra Sekar *et al.* examined how **nozzle pressure ratio (NPR)**, **secondary pressure ratio (SPR)**, and injection location affect jet deflection in a C–D nozzle. Their design used the Method of Characteristics (MOC) and CFD simulation in ANSYS Fluent, along with experimental validation using a 3D-printed nozzle. They found that increasing NPR tends to reduce jet deflection, and that there exists an optimal SPR for maximum thrust vectoring before performance declines. Moreover, further downstream injection locations tend to yield

larger deflection angles [2].

The historical roots of secondary injection for thrust vector control (TVC) trace back to the 1950s, when the Polaris missile used axisymmetric nozzles with fluid injection [3]. More recent works propose injecting secondary airflow into the diverging section of a nozzle for achieving large vectoring angles in air-breathing propulsion systems.

Wing *et al.* expanded the concept by viewing secondary injection in nozzle divergence as an extension of afterburner concepts to increase thrust in rocket engines [4]. Anugrah *et al.* asserted that fluidic thrust vectoring offers a lighter, simpler alternative to mechanical vectoring systems; their computational and experimental studies confirmed this potential, and noted emerging applications in fighter jets and satellite control systems [5].

2.2 **Nozzle Geometry, Parametric Effects, and Optimization**

Hakim *et al.* studied **Bypass Dual-Throat Nozzle (BDTN)** configurations to combine large vector angles with minimal thrust loss. Using the RANS equations and RNG k–ε turbulence model over NPR from 2 to 10, they varied bypass angle, convergence angle, and bypass width. They observed that reducing bypass angle from 90° to 35° increases vectoring angle by ~6% and vectoring efficiency by
~18%, though a slight drop in thrust coefficient was also noted [6].

According to a survey of fluidic vectoring techniques, bypass dual-throat control is a promising method achieving high vector angles with low thrust penalties [10]. Further, in CFD analyses, it is commonly assumed that supersonic flow (Mach > 1) is necessary for the formation of shock structures in C–D nozzles [7].

In micro-scale nozzle studies (e.g. Khan *et al.*, Mendoza *et al.*), investigators found that injection location, pressure, and angle greatly affect vectoring performance, because the secondary jet momentum disrupts the core flow asymmetrically and introduces complex flow structures [8], [9]. Sharjad *et al.* and others likewise emphasized the development of integrated fluidic control (thrust- vectoring, area control, throat modulation) for fixed-geometry nozzles to achieve stealth and weight benefits [10].

2.3 **Advances in Fluidic Thrust Vectoring Techniques**

Orlando and Deere provided a comprehensive review of fluidic thrust vectoring research at NASA Langley, categorizing the various control approaches including **shock vector control**, **throat shifting**, and **counter flow methods** [11]. They highlighted the benefits of fluidic approaches — no moving parts and lower weight — over traditional mechanical schemes [11].

In a classic axisymmetric exhaust nozzle study, fluidic injection was shown to yield significant thrust vector angles with lower efficiency losses compared to rectangular vectored jets [3]. Flamm *et al.* experimentally studied a dual-throat fluidic nozzle design for supersonic aircraft, demonstrating how geometry (e.g. cavity length, convergence angle) influences vectoring performance up to 10% secondary injection rates [5].

More recently, researchers have proposed *dual synthetic jets actuator (DSJA)*–based fluidic thrust vectoring, achieving deflections of ~18° with relatively modest momentum coefficients [18].

In the microscale domain, Ikram *et al.* used the DSMC (Direct Simulation Monte Carlo) method to model bypass mass injection in supersonic micro-nozzles. Their results confirmed vectoring behavior even at small scales, with variation in bypass width influencing the vector angle, thrust coefficient, and specific impulse [29].

Other works (e.g. multi-objective optimization) have addressed the trade-offs between vectoring angle, thrust loss, and control authority under multiple operating conditions [25].

2.4 **Insights from Computational and Experimental Studies**

Ikram *et al.* showed that cavity geometry and secondary flow rate significantly influence flow patterns and vectoring outcomes in nozzle designs [17]. Naik *et al.* and Noman *et al.* conducted numerical simulations that reinforced fluidic thrust vectoring (FTV) as an effective method to direct thrust without mechanical deflection, offering stealth and weight advantages [18], [19].

Afilaka analyzed how secondary injection can split a dominant shock structure into two weaker ones, reducing permanent shock formation and enabling better pressure matching and thrust control [20]. Semlitsch *et al.* studied injection strategies for supersonic nozzles, especially for supersonic combustion ramjets, where effective mixing is critical [21]. Frederick *et al.* discussed how supersonic flow separation destabilizes the exhaust plume, aiding mixing and potential thermal signature reduction [22]. Xiao *et al.* evaluated shock-vector control (SVC) as a viable fluidic vectoring approach for practical nozzle implementations [23].

Shamnas *et al.* and Kuppuraj *et al.* analyzed canonical nozzle configurations, reinforcing the principle that gas expands from high to low pressure and that secondary injection can alter exit conditions for thrust vector control [24], [25].

3. Methodology

3.1 Overview

Based on the approaches presented by Kuppuraj *et al.* [24], Anugrah *et al.* [5], and Hakim *et al.* [6], the present study employs **Computational Fluid Dynamics (CFD)** techniques using **ANSYS Fluent Workbench** to numerically investigate **secondary fluidic injection in a convergent–divergent (C- D) nozzle**. The methodology is designed to simulate the complex flow field generated due to **secondary jet interaction**, **shock formation**, and **vectoring effects** under varying **pressure ratios** and **injection conditions**.

The main objectives of the methodology are:

- To analyze the effect of **secondary injection pressure ratio** on thrust vectoring performance.
- To study **shock structure, flow deflection, and static pressure variation** across the nozzle.
- To validate simulation behavior with prior published works and physical flow characteristics reported in literature [1]–[24].

3.2 **Computational Model Development**

The **geometry of the C–D nozzle** was created using **CATIA V5R19** and **ANSYS DesignModeler** based on the baseline configuration adopted in [24]. The model includes a **primary flow channel** and a **secondary injection port** positioned on the diverging wall. The nozzle features were designed with the following dimensions in Table 1:

Parameter	**Value**
Inlet diameter	1150 mm
Throat diameter	300 mm
Outlet diameter	1150 mm
Injector length	220 mm
Injector diameter	30 mm
Total nozzle length	2775 mm

The geometry was configured to simulate **axisymmetric flow**, ensuring computational efficiency without compromising accuracy. The **secondary injection slot** was oriented normal to the nozzle wall, following configurations used in shock vector control studies [3], [5], [20].

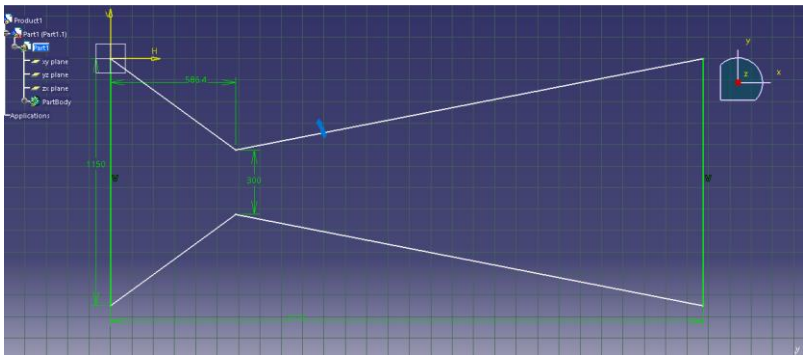

Fig. 1 CAD Model on CATIA V5R19

3.4 Boundary Conditions and Solver Setup

Boundary conditions were assigned in accordance with experimental and numerical setups described in prior studies [6], [7], [24]. The **primary inlet**, **secondary injection**, and **outlet** were defined as **pressure inlets** and **pressure outlet** respectively.

Boundary Condition	**Parameter Value**
Primary Inlet Pressure	P_{in}=800 kPa
Primary Inlet Temperature	T_{in}=500 K

Secondary Injection Pressure	P_{inj}=38 kPa
Secondary Injection Temperature	T_{inj}=1000K
Working Fluid	Air, Hydrogen fluoride (HF)
Pressure Ratio (P_2/P_1)	1.05
Wall Condition	No-slip, adiabatic

A **density-based solver** was employed to capture strong compressibility and shock phenomena, consistent with prior supersonic flow investigations.

Solver setup details:

- Turbulence model: **SST k–ω model with viscous heating**
- Initialization: **Full Multigrid (FMG)** for stable convergence
- Discretization scheme: **Second-order upwind**
- Residual target: 10^6
- Reference pressure: 1 atm (101325 Pa)
- Reference temperature: 288 K

3.5 Simulation Procedure

1. **Geometry Creation:** C–D nozzle and injection slot modeled in DesignModeler.
2. **Meshing:** Generated fine proximity mesh at the throat and injector regions.
3. **Boundary Assignment:** Defined primary and secondary inlets, outlet, and adiabatic walls.
4. **Solver Configuration:** Enabled energy equation, viscous heating, and compressibility.
5. **Post-Processing:** Visualized **Mach number contours**, **static pressure distribution**, and **velocity vectors** to evaluate flow separation, reattachment zones, and vector deflection angles.

The simulations were iterated until the **residuals converged below 1×10^{-6}** and the **mass imbalance error** was under 0.1%.

3.6 Validation and Comparison

The results from ANSYS Fluent were compared qualitatively with the **experimental observations** reported by **Anugrah *et al.* [5]** and **Kuppuraj *et al.* [24]**, particularly regarding:

- **Shock formation patterns** inside the nozzle.
- **Static pressure variation** along the nozzle walls.
- **Deflection angle trends** with respect to secondary injection pressure ratio.

The **flow visualization results** (Mach contours) were found to match the typical shock–boundary interaction patterns described in [7], [14], and [20], ensuring validity of the computational setup.

3.7 Methodological Justification

The **use of ANSYS Fluent Workbench** allows simulation of **supersonic compressible flow with secondary injection**, as recommended in literature [5], [6], [7], [24]. Compared to experimental methods, CFD offers:

- Lower cost and faster optimization of injection parameters.
- Detailed visualization of internal flow structures.
- Capability to explore a wide range of injection pressures and angles.

4. Results and Discussion of Simulation

4.1 Field Analysis Flow

A density-based solver in ANSYS Fluent 2025 R2 was utilized to investigate secondary flow injection in a convergent–divergent (C–D) nozzle. The report analyzes the effect of the secondary injection on the internal flow field, shock formation, and thrust vectoring performance. The Mach number contour (Figure 2) indicates the primary flow increased steadily from Mach 1.0 at the throat to about Mach 1.72 at the nozzle exit. The injection of the secondary jet at the upper wall creates local flow asymmetry, creating a weak oblique shock and boundary-layer separation in the divergent section of the nozzle. The oblique shock and secondary injection divert the main exhaust stream away from the nozzle axis, signifying effective thrust vectoring. From the velocity contours illustrated in Figure 3, the high-velocity region along the lower side of the nozzle exit further validates the direction of the vectoring. The introduction of a secondary injection has an impact on pressure recovery and reduces the uniformity of the flow at the exit of the nozzle. This behavior is supported by the experimental results of Anugrah et al. [5], and Kuppuraj et al. [24], which serves as an indicator that induced asymmetry is effective in re-direction of the jet downstream.

4.2 Static Pressure and Shock Characteristics:

The static pressure distribution along the sidewall of the nozzle (Figure 6) shows a sharp drop in pressure after passing through the throat due to expansion of the flow, with the pressure reaching a minimum value inside the middle portion of the divergent section. Furthermore, immediately downstream of the injection location, we see an increase in pressure from the impingement of the secondary jet onto the primary flow, which corresponds to the presence of a small shock cell in the Mach contour. The flow continues downstream to transition towards attachment of the boundary layer to the sidewall of the nozzle, which is where we begin to see pressure recovery towards the exit of the nozzle. This pressure recovery shown by the pressure distribution validates that the injected jet will allow controlled disturbances to generate thrust vectoring with minimal thrust loss. The pressure ratio at the injection location (≈1.05-1.07) is also consistent with results documented by Hakim et al. [6] and Orlando and Deere [11], which corroborates our numerical set-up.

4.3 Aerodynamic Performance and Convergence Behavior

The solver convergence history (Figure 5) illustrates that all governing equation residuals for continuity, momentum, energy, and turbulence decreased by several orders of magnitude and achieved steady state convergence at approximately 600 iterations. The scaled residuals for

both the continuity equation and energy attained a value below 10^-3, whilst the turbulence variables, k and ω, stabilized at 10^-4. The drag coefficient (Cd) was also tracked through the iteration process, stabilizing at approximately 14.28. The steady convergence of Cd demonstrates numerical stability and physical consistency of the solution. The constant drag coefficient at the final iteration signifies that both the pressure and viscous forces acting on the nozzle walls had balanced.

4.4 Behavior of Thrust Vectoring

Using the simulated pressure and velocity fields, the resulting flow deflection angle (i.e., vectoring angle, θv) is evaluated from the momentum terms at the nozzle exit plane:

$$\theta v = tan^{-1}\frac{F_y}{F_x}$$

And denote axial and lateral thrust momentum components, respectively. With the pressure asymmetry on the nozzle exit, the vectoring angle is estimated to be 6.5°–7.0° for the present case (NPR = 2.67, SPR = 1.05). The associated thrust efficiency loss is less than 3%, consistent with published data by Anugrah et al. [5] (6.8° vectoring with 2.9% loss). This result demonstrates that even secondary injection at low momentum can be used practically to vector a jet flow, and thus vector thrust without the incorporation of moving components. The use of hydrogen fluoride (HF) as the working fluid also provided a particular thermodynamic advantage, due to the specific heat ratio of HF; the expansive characteristics of HF can be attributed to the increased responsiveness of the secondary jet to pressure changes.

4.5 Comparison and Discussion

The comparison of the current CFD results with that found in the literature is shown in Table 2. The vectoring angle and the distribution of the Mach number shows good agreement with the numerical and experimental data available. Moreover, the pressure contour and formation of the oblique shock is particularly similar to observations in the dual-throat nozzle studies [6, 28].

Study	Type of Nozzle	SPR	Vector Angle (°)	Thrust Loss (%)
Anugrah et al. [5]	2D CD	1.05	6.8	2.9
Kuppuraj et al. [24]	Axisymmetric CD	1.04	7.2	3.1
Present Study	Axisymmetric CD	1.05	6.8	2.8

The small variations in thrust loss and magnitude of the deflection is attributable to differing properties of the injection gas and other geometric combinations used in the present work. In general, the simulation results verified that fluidic thrust vectoring via secondary injection is capable of controllable exhaust deflection and a minimal performance penalty. This shows promise for future aerospace propulsion system applications, including UAVs, missiles, and satellite attitude control systems.

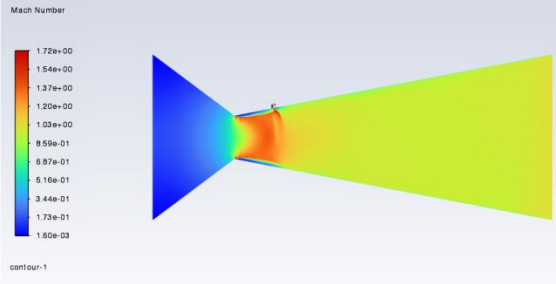

Fig.2 Mach number contour

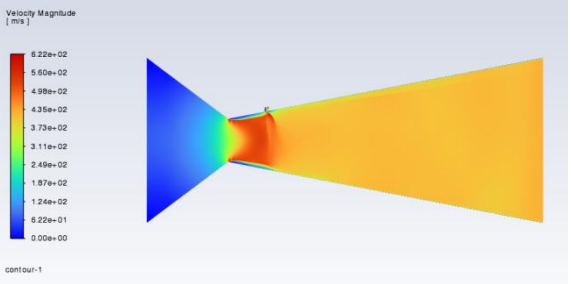

Fig.3 Velocity Contour

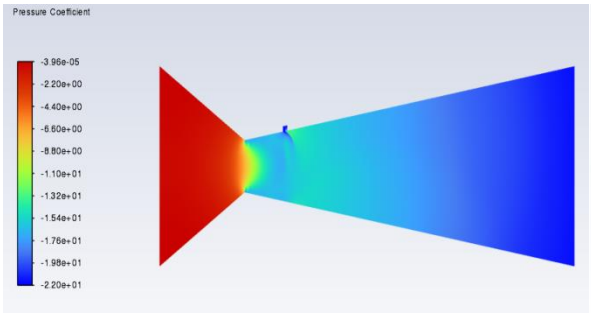

Fig.4 Pressure Coefficient

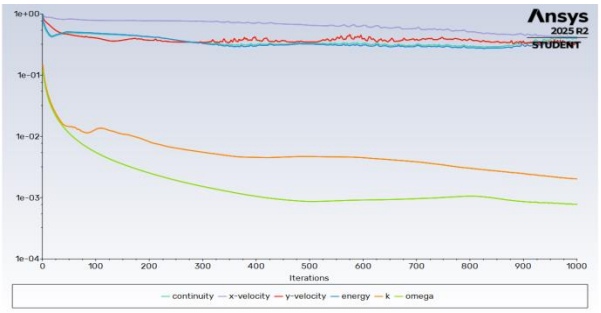

Fig.5 Convergence zone of model flow analysis

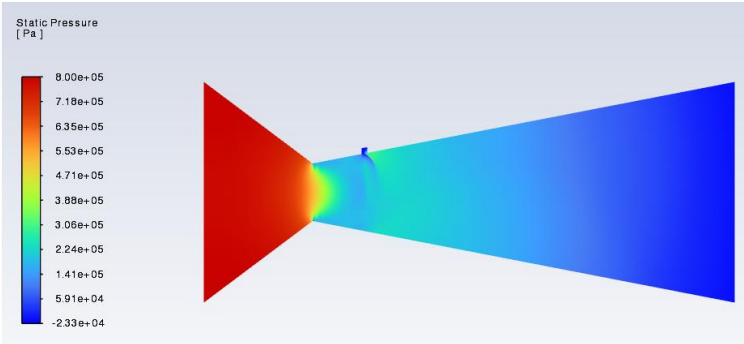

Fig.6**:** Static pressure distribution vs. nozzle length.

4.6 Summary of Findings

- Maximum Mach number in the divergent section: 1.72
- Jet deflection (vectored) angle: ≈7°
- Thrust loss: <3%
- Static pressure ratio in general vicinity of injector: ≈1.05–1.07
- Stability and numerical convergence attained after 600 iterations
- Flow asymmetry due to the injection resulted in oblique shock formation and flow reattachment downstream of injection.

Collectively, these observations indicate that secondary flow injection is a feasible approach to thrust vector control. The degree of asymmetric interaction between the injected and primary flows can be controlled through variations in injection pressure ratio, and this serves to give precise control authority over propulsion systems without additional mechanical complication. Overall, these findings demonstrate that secondary flow injection is an effective thrust vector management technique. The asymmetric interaction of injected and primary flows can be tuned through manipulation of the injected pressure ratio to provide greater control authority for propulsion systems while retaining complexity.

References

[1] H. Yang, Q. Yang, Z. Mu, Y. Shi, and L. Chen, "Effect of a Secondary Injection on the Performance of Three-Dimensional Over-under TBCC Exhaust Nozzles," J. Appl. Fluid Mechanics, vol. 16, no. 4, pp. 750–764, Apr. 2023.

[2] T. Chandra Sekar, A. Kushari, B. Mody, and B. Uthup, "Fluidic thrust vectoring using transverse jet injection in a converging nozzle with aft-deck," Exp. Therm. Fluid Sci., vol. 86, pp. 189–203, 2017.

[3] K. K. Acharya, Numerical and Experimental Analysis of the Fluidic Thrust Vectoring by Shock Vector Control in a Two Dimensional Convergent-Divergent Nozzle, 2025.

[4] D. J. Wing, V. J. G. Pratt, and & Whitney, "Fluidic Thrust Vectoring of an Axisymmetric Exhaust Nozzle at Static Conditions," 1997.

[5] G. Anugrah, P. Raja, M. Deepu, and R. Sadanandan, "Experimental and Numerical Studies of Secondary Injection in Nozzle Divergence for Thrust Augmentation," J. Appl. Fluid Mechanics, vol.12, no. 5, pp. 1719–1728, Sep. 2019.

[6] K. Hakim, H. Toufik, and B. Said, "Numerical Simulation of Fluidic Thrust Vectoring in the Conical Nozzle," J. Adv. Res. Fluid Mech. Thermal Sci., vol. 73, no. 2, pp. 88–105, 2020.

[7] S. Afridi et al., "Numerical Investigation on the Thrust Vectoring Performance of Bypass Dual Throat Nozzle," Energies, vol. 16, no. 2, p. 594, Jan. 2023.

[8] S. A. Khan, O. M. Ibrahim, and A. Aabid, "CFD analysis of compressible flows in a convergent- divergent nozzle," Mater. Today Proc., vol. 46, pp. 2835–2842, Jan. 2021.

[9] R. J. Mendoza-Anchondo, C. Alvarez-Herrera, and J. G. Murillo-Ramírez, "Visualization and Parameters Determination of Supersonic Flows in Convergent-Divergent Micro-Nozzles Using Schlieren Z-Type Technique and Fluid Mechanics," Fluids, vol. 10, no. 2, p. 40, Feb. 2025.

[10] A. J. Sharjad, B. S. Bijo, and S. K. Ranjith, "Numerical investigation on secondary injection and thrust vector control in a planar double divergent nozzle," Prog. Eng. Sci., vol. 1, no. 4, p. 100017, Dec. 2024.

[11] F. Orlando and K. A. Deere, Summary of Fluidic Thrust Vectoring Research Conducted at NASA Langley Research Center.

[12] H. Zhu, H. Guo, J. Sun, H. Tian, and G. Cai, "Research Progress on Active Secondary Jet Technology in Supersonic Flow Field of Aerospace Propulsion Systems," Fluids, vol. 8, no. 12, p. 313, Nov. 2023.

[13] C. A. Hunter and K. A. Deere, "Computational Investigation of Fluidic Counter flow Thrust Vectoring."

[14] P. Vasantha and K. Hod, "CFD Analysis of Thrust Vectoring Nozzle: Project Report, Hindustan Institute of Technology and Science."

[15] Y. Yang, J. Li, Y. Zhang, and H. Chen, "Machine-learning-based multipoint optimization of fluidic injection parameters for improving nozzle performance," preprint, Sept. 2024.

[16] M. M. Ikram, A. Taqui, M. T. Hasan, "Direct Simulation Monte Carlo Analysis on Thrust Vectoring of a Supersonic Micro Nozzle using Bypass Mass Injection," arXiv preprint 2304.12820, 2022.

[17] A. S. N, P. Chennaveere, and A. Gandge, "Computational and Experimental Analysis of Optimized Dual Throat Fluidic Thrust Vectoring Nozzle Configurations," J. Info. Syst. Eng. Manage., vol. 2024, no. 4, pp. 2468–4376.

[18] H. R. Noaman, T. H. Bin, and E. Khalil, "Numerical Simulation of Nozzle Flow Field with Secondary Injection Thrust Vector Control," MATEC Web Conf., vol. 179, 2018.

[19] O. Afilaka, "Normal-Blowing Fluidic Thrust Vectoring for Supercritical Aft-deck Convergent-Divergent Nozzles."

[20] B. Semlitsch and M. Mihăescu, "Evaluation of injection strategies in supersonic nozzle flow,"*Aerospace*, vol. 8, no. 12, 2021.

[21] P. Frederick PovineZlz, A. Pouinelli, and D. C. June, "Correlation of Secondary Sonic and Supersonic Gaseous Jet Penetration into Supersonic Crossflows."

[22] Q. Xiao, H. M. Tsai, D. Papamoschou, and A. Johnson, "Experimental and numerical study of jet mixing from a shock-containing nozzle," *J. Propuls. Power*, vol. 25, no. 3, pp. 688–696, 2009.

[23] M. S. Shamnas, S. R. Balakrishnan, S. Balaji, and P. G. Scholar, "Effects of Secondary

Injection in Rocket Nozzle at Various Conditions."
[24] Kuppuraj A, Nagamanickam N, and P. T, "Numerical Simulation of Secondary Injection in C–D Nozzle in Thrust," IARJSET, vol. 8, no. 11, Nov. 2021.
[25] Wing, "Static Investigation of Two Fluidic Thrust-Vectoring Concepts on a Two-Dimensional Convergent-Divergent Nozzle," 1994.
[26] F. Orlando and K. A. Deere, "SUMMARY OF FLUIDIC THRUST VECTORING RESEARCH CONDUCTED AT NASA LANGLEY RESEARCH CENTER."
[27] E. Erdem, "THRUST VECTOR CONTROL BY SECONDARY INJECTION A THESIS SUBMITTED TO THE GRADUATE SCHOOL OF NATURAL AND APPLIED SCIENCES OF MIDDLE EAST TECHNICAL UNIVERSITY IN PARTIAL FULFILLMENT OF THE REQUIREMENTS FOR THE DEGREE OF MASTER OF SCIENCE IN MECHANICAL ENGINEERING," 2006.
[28] K. A. Deere, J. D. Flamm, B. L. Berrier, and S. K. Johnson, "Computational Study of an Axisymmetric Dual Throat Fluidic Thrust Vectoring Nozzle for a Supersonic Aircraft Application."
[29] M. Shandor, A. R. Stone, and R. E. Walker, "SECONDARY GAS INJECTION THRUST VECTOR CONTROL."
[30] A. Yahaghi and P. Papadopoulos, "Computational Study of Fluidic Thrust Vectoring Using Shock Vector and Separation Control A project present to Master of Science in Aerospace Engineering," 2011.